PROBA-3 Formation Flying High Performance Control

R. Sánchez-Maestro[(1)], **A. Agenjo-Díaz**[(2)], **and A. Cropp**[(3)]
[(1)]*SENER, C/ Severo Ochoa 4, Tres Cantos (Madrid), Spain, +34 918077189, raul.sanchez@sener.es*
[(2)]*SENER, C/ Severo Ochoa 4, Tres Cantos (Madrid), Spain, +34 918077381, alfredo.agenjo@sener.es*
[(3)]*ESA-ESTEC, TEC-ECN, Keplerlaan 1, Noordwijk, The Netherlands, +31 715658797, alexander.cropp@esa.int*

Abstract: *PROBA-3 is the most challenging of the ESA's technology demonstration missions and is devoted to fly for the first time a fully autonomous Formation Flying (FF) mission. It will require overcoming several difficulties ranging from the development of new technologies, to the application of advanced and robust control techniques and implementation of a full on-board autonomy for nominal FF manoeuvres. The main mission challenge is to keep the S/C formation, which functions as a virtual rigid structure acting as a coronagraph, with very high pointing and positioning precision. This will be done near apogee with an advanced GNC system that uses μm precision optical metrology and mN thrusters. This paper shows the H_∞ design process for the high performance relative position control during the formation flying station keeping and manoeuvres.*

Keywords: *Formation Flying, H_∞ synthesis, MIMO control system, Elliptic orbit.*

1. Introduction

1.1. Mission Overview

PROBA-3 (PRoject for On-Board Autonomy) is the most complex and ambitious of the ESA's technology demonstration missions and it is part of the overall in Orbit Demonstration missions from the ESA Technical Directorate. The main objective of PROBA-3 is to demonstrate precision Formation Flying techniques and technologies as precursor to future ESA missions.

The PROBA-3 System consists of two independent 6DoF (Degrees of Freedom) spacecraft flying in a high elliptic Earth orbit with the perigee and apogee at respectively 6.971 km and 66.901 km. The nominal master from GNC point of view is the Occulter Spacecraft (OSC) since it is the spacecraft that performs the fine actuations with Cold Gas thrusters for the relative position. The reference for the active spacecraft is the Coronagraph Spacecraft (CSC), which carries the relative position metrology system. These two spacecraft will autonomously break and reacquire the formation at each perigee pass and demonstrate formation flying near apogee. The combined system is expected to achieve a relative positioning accuracy of the order of 1mm over a separation range of 25m to 250m.

1.2. Performance Requirements

The tables 1 and 2 show a summary of the values for the Relative Displacement Error (RDE), the Absolute Attitude Error (AAE) and the Absolute Attitude Measurement Error (AAME). The RDE requirements belong to a set of requirements, the so-called HPAP

(High-Precision Attitude and Position), which have been defined to include the maximum desirable precision on attitude and relative position for the PROBA-3 mission. Note that the lateral displacement error has been assumed to be scaled approximately with the relative Inter-Satellite Distance (ISD) between the two spacecraft. The HPAP requirements are applicable to the nominal fine station keeping (FSK) phase, which are either inertial or Sun pointing. During the experimental retargeting and resizing manoeuvres, the relative position control requirements are somewhat relaxed and are subject to the HPM requirements (High Performance during Motion). However, the more stringent HPAP requirements are still applicable to the attitude control during these manoeuvres.

Table 1: PROBA-3 Relative Positioning Performance Requirements

Error	HPAP Requirement (1σ)			HPM Requirement (1σ)
	ISD ≤ 40m	40m < ISD ≤ 160m	160m < ISD ≤ 250m	
RDE_X (Longitudinal)	1.5 mm	1.5 mm	1.5 mm	2.5 mm
$RDE_{Y,Z}$ (Lateral)	0.5 mm	0.73 mm	1.2 mm	2.5 mm

Table 2: PROBA-3 Attitude Pointing Performance Requirements

S/C	Error	Attitude Pointing Requirement (1σ)
CSC	AAE_X (Around LOS)	300 arcsec
	$AAE_{Y,Z}$ (Across LOS)	2.8 arcsec
	$AAME_X$ (Around LOS)	30 arcsec
	$AAME_{Y,Z}$ (Across LOS)	1.25 arcsec
OSC	AAE_X (Around LOS)	900 arcsec
	$AAE_{Y,Z}$ (Across LOS)	30 arcsec
	$AAME_X$ (Around LOS)	300 arcsec
	$AAME_{Y,Z}$ (Across LOS)	5 arcsec

1.3. GNC General Architecture

The GNC for both PROBA-3 spacecraft is to be separated into two interconnected GNC modules, designed together, although implemented by different companies, and integrated by SENER and commanded from only one brain within the GNC software. These two GNC modules are the Formation Flying GNC (FF-GNC, in charge of relative position control) and the Spacecraft GNC (SC-GNC, in charge of attitude control and low level actuator commanding). The modes, states and the schedule in both modules are controlled by the Formation Flying Management (FFM). The overall responsibility for the FF Software, including the development of FFM and FF-GNC has been assumed by GMV (Spain) with SENER as subcontractor being responsible for the control design (FF-C) and FF-FDIR. The responsibility for SC-GNC has been assumed by NGC Aerospace (Canada) following a specification by SENER.

- The FF-GNC includes all the functions for the state determination, guidance profile computations and control laws of the formation translation (relative position). It receives from SC-GNC the absolute attitude data for inclusion in the FF-N module.
- The SC-GNC includes the classical functions of an Attitude and Orbit Control system (AOCS), with absolute attitude determination, absolute attitude control, and actuators low level commanding. Additionally, it includes the absolute position and velocity determination, which is sent to the FF-GNC when needed.

  (Note, however, that the FF-GNC is the main user of the thruster system during the flight formation phase. Consequently, the thruster actuator manager function acts according to the specifications set by the needs of the FF-C).

This separation, which is treated as a design constraint, is a choice made by the industrial organisation of PROBA-3 motivated by the mission characteristics, where the two spacecraft must be able to be operated in stack configuration and separately, where the SC-GNC is commanded by ground without the FF-GNC and FFM in the loop. The nominal mission includes all modules working together in the control loop to demonstrate the Formation Flying capability.

Two main distinct manoeuvres to be performed can be distinguished, which are denoted as the rigid and loose manoeuvres.

- Rigid manoeuvres: where the nominal attitude profile for each spacecraft has to keep the two payload reference coordinate frames parallel during the whole manoeuvre in such a way that the high-accuracy metrology system is able to operate throughout these manoeuvres. The formation will either change the distance between spacecraft (resizing: from 150m to 25m and back and from 150m to 250m and back) or the formation is rotated (retargeting up to 30 degrees and back to the original position) or both simultaneously.
- Loose manoeuvres: There are no stringent requirements on attitude and position to be met during the manoeuvre, only at the start and end of the manoeuvre. These manoeuvres will be performed with impulsive ΔVs calculated in the Guidance module.

These manoeuvres implying relative position change will be executed by the OSC spacecraft that carries the mN thruster system. The relative position measurements are taken by CSC and transmitted to the OSC via radiofrequency with an Inter Satellite Link (ISL).

2. Control Design

The Guidance module will provide a position and attitude profile, which is compared to the Navigation results. In order to improve the response and performance during FSK and particularly the manoeuvres, the controller consists of both a feed-forward term and feed-back term. The feed-forward terms are derived directly from the Guidance profiles and consist of the nominal forces and torques that are necessary to execute the manoeuvre. The feed-back term then compensates for any deviations from the nominal path.

For the FF-GNC control, the most demanding manoeuvres are the rigid ones, where the high accuracy metrology with its narrow field of view is operational. Throughout these rigid manoeuvres, only one spacecraft will be subject to active closed-loop position control while both spacecraft will be actively controlled to keep the attitude profiles as provided by the guidance modules. This scheme is applicable for the distinct formation cases where the attitude and ISD vector have to be kept inertial, Sun pointing and during a retargeting manoeuvre.

Modern robust control techniques, such as H_∞ and μ-analysis, will be used to design and analyse the FF-GNC controller. The relative orbital dynamics for elliptic orbits are modelled and used as the plant model. A very important non-linear element is the presence of thrusters and its effects are carefully taken into account by designing an adequate modulation scheme and by making sure that the H_∞ design does not enter the frequency range of the modulation. Naturally, the attitude and position control are not completely independent from each other for the formation control scheme. A GNC architectural separation of attitude and position exists hence the attitude dynamics is taken into account in the FF-GNC design by both imposing performance requirements on the SC-GNC and to add the necessary robustness properties to the position controller synthesis and analysis.

2.1. Coupling between position and attitude

At system level, the decision has been made to separate the position and attitude control, which are respectively executed by the FF-GNC and SC-GNC. In fact, due to how the industrial organisation is set up, they are both designed by different parties hence a combined and strict 6DoF approach is discarded. Nevertheless, the reality is that there is an inevitable coupling between the attitude and position dynamics hence a strict separation and independent design is not possible and some iteration between both parties is mandatory during the design and analysis process. In order to cope with the coupling and to minimise its effect, the following two measures are introduced. First, both attitude and position control are subject to requirements and restrictions such that they interact as little as possible with each other. Second, the attitude control is included in the position control design as a perturbation source within the H_∞ robust design framework.

The most important requirement is to have different controller bandwidths for the position and attitude control in order to avoid any dynamical interaction leading to any undesired amplification of position or attitude dynamics. The attitude control is assumed to be significantly faster than the position control. Consequently, any attitude related effects will behave as a high frequency disturbance.

Ideally, when firing the thrusters, they would generate pure forces. But the presence of thruster errors and mass centre uncertainties and variations there will be residual perturbation torques that will affect the attitude. Consequently, the design of the position control should take this into account by avoiding large control forces and too much control activity. This way, the attitude dynamics will be perturbed less allowing the attitude controller to compensate for these impulsive thruster based torque perturbations.

2.2. Plant modelling

In this particular mission, the flight formation is defined wrt to quasi-inertial space and for this reason one could particularise the dynamics and formulate a plant expressed in the inertial frame. However, many flight formation and rendezvous problems are treated wrt to a LVLH (Local Vertical Local Horizontal) frame so that would be a natural option as well. In principle, the inertial approach may seem tempting due to some problem specific simplifications but the LVLH formulation has been chosen, mainly for the following reason: one of the objectives of PROBA-3 is to obtain a design approach and philosophy for future applications and the LVLH approach is considered to be more general and applicable to other flight formation scenarios.

PROBA-3 consists of two spacecraft in a high elliptic orbit around the apogee hence the governing linearised equations according to Reference [2] is a LTV (Linear Time Varying) system since the orbital rate is varying depending on the position within the orbit. The synthesis procedure requires a LTI (Linear Time Invariant) system and to obtain this, the instantaneous system with fixed parameters corresponding to a reference point within the orbit is selected. Naturally, the further this reference point moves from the apogee, the larger the local orbital rate and the stronger the gravity gradient and associated MIMO cross couplings of the in-plane orbital motion. As a conservative value, the true anomaly of the reference point is chosen to be around 5 deg less than that of the orbital arc corresponding to the formation flying phase (see Fig. 1). The rationale is that the resulting synthesised controller is able to cope with stronger relative dynamical effects although care must be taken during the synthesis procedure that the controller does not “blindly” incorporate the reference relative orbital dynamics through inversion thus relying explicitly on the presence of those cross coupled dynamics.

In any case, once the controller is synthesised, a post-analysis is performed covering several LTI plant models, each corresponding to a different point along the flight formation orbital arc, in order to check whether the constraints imposed by the weighting functions within the H_∞ framework are not violated.

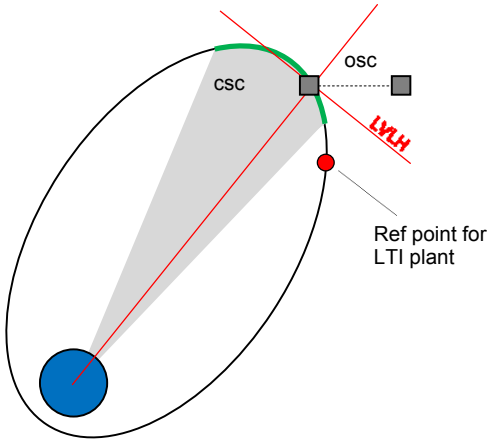

Fig. 1: Symbolic representation of the flight formation phase

2.4. Combination of feedback and feed-forward term

The relative orbital dynamics are an issue of major importance and the controller needs to be able to compensate for any perturbation caused by these dynamics. But these dynamics are deterministic and they can in theory be compensated in open loop by adding a feed-forward force term by estimating on-line the gravity gradient acceleration. This approach has the benefit that the resulting controller (combination of feed-back and feed-forward) is more responsive, has faster convergence and may in principle alleviate the requirements on the design criteria of the feedback term. This combination is in fact the adopted design philosophy for the PROBA-3 controller.

However, to be conservative and as a worst case scenario, the feedback controller synthesis is performed with the assumption that it has to compensate the gravity gradient without any external aid such as this feed-forward term. The main impact is that the feedback term will thus contain more integral action with the explicit aim of rejecting the low-frequency gravity gradient perturbation. The feed-forward term can therefore be considered a “bonus” that should further improve the performance.

2.5. H_∞ Synthesis

The final objective is to design a robust controller based on H_∞ synthesis and μ-analysis. The design process starts by analysing the control problem and adapting it to the H_∞ framework where a generalised plant model is obtained with a set of suitable weighting functions. For now, a controller is designed without explicitly taking into account all uncertainties for robustness properties. This task is left for a later phase when the PROBA-3 mission gains in maturity and when certain GNC related issues become more consolidated allowing for a proper assessment of the relevant robustness requirements and quantifications.

The current aim is to set up the H_∞ design environment, adapt the PROBA-3 high performance control problem to the H_∞ framework and to synthesise a controller that meets the performance requirements under nominal conditions in a sufficiently representative simulation environment without going into detail regarding Robust Performance (RP) and Robust Stability (RS), which are design objectives left for future phases. A block diagram of the feedback system and weighting functions is shown below in Fig. 2

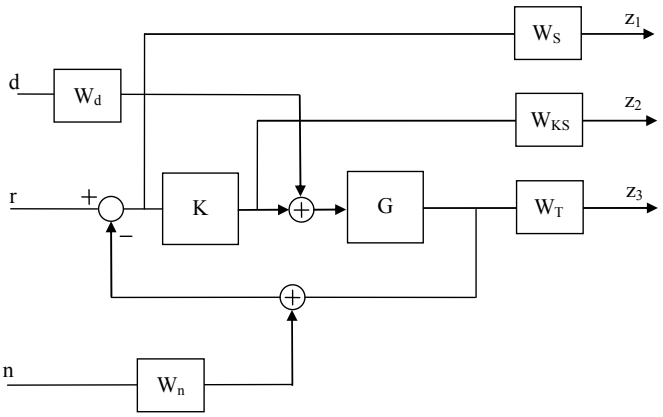

Fig. 2: Feedback block diagram with the weighting functions for the H_∞ synthesis

Here the objective is to synthesise a controller K such that the H_∞ norm from the inputs d, r and n to the outputs z_1, z_2 and z_3 is close to 1 through scaling. The weighting functions W_i are to be tuned and scaled adequately in order to obtain the desired properties of the closed loop system. A description of the function blocks and variables is given next:

- d This input represents the disturbance force. In this scheme it mainly contains the low frequency differential solar radiation pressure force. (Note that the gravity gradient perturbation is already included in the plant model G).
- r This is the tracking reference command. (Since the plant G contains the relative orbital dynamics centred at the CSC, this input is thus used to "tell" the synthesis procedure at what distance the OSC is to be maintained thus determining the necessary integral action to cope with the gravity gradient).
- n This input represents the noise of the Navigation filter.
- K Controller to be synthesised.
- G Plant model describing the relative orbital dynamics according to the equations in Reference [2].
- W_T This weighting function bounds the complementary sensitivity function T and is here primarily used to set an upper limit of the bandwidth, which is critical in the presence of the thruster PWM. Additionally, it can be used to include robustness properties but that aspect is excluded in the current design process.
- W_S This weighting function bounds the sensitivity function S and it is here primarily used to impose a desired suppression factor to the low frequency external disturbance forces such as the solar radiation pressure and gravity gradient.
- W_{KS} This weighting function bounds the maximum values of the control commands. In this particular case, this function is primarily used to add additional poles and zeros to the controller transfer function for smoothing purposes of the control error signal.
- W_d This weighting function represents the magnitude scaling and frequency range of the external disturbance forces. Here, the main disturbance of interest is the differential solar radiation pressure force.
- W_n This weighting function represents the magnitude scaling and frequency range of the Navigation errors.

Since there are 3 inputs and 3 outputs, there are a total of 9 combinations of individual transfer functions. However, it is not possible to tailor the weighting functions and scale them independently for each individual combination. Instead, the emphasis will be put on the input/output transfer functions from r to all 3 outputs and from d to z_1. Nevertheless, the scaling and tuning is done such that none of the other combinations introduce any "conflicts" in the sense that the nominal ideal H_∞ norm of 1 cannot be met and afterwards, a check is to be performed to analyse the norm and to assess whether they influence the synthesis result. When tuning the weighting functions, the following criteria have been followed:

- Bandwidth upper limit: At present, a thruster PWM period of 20 seconds has been chosen. Based on this value, the W_T function is tuned accordingly so that the bandwidth is sufficiently lower than the PWM frequency. The upper bound of

the control bandwidth is determined by the cross-over frequency of the W_T function, which is modelled by a 1st order transfer function.

- Suppression of the differential solar radiation pressure: This suppression is accomplished by tuning the channel from input *d* to output z_1. The weighting functions of relevance are W_d and W_S. The former contains the information regarding the magnitude of said perturbation and the frequency range within which it operates. The magnitude is set according to the maximum expected perturbation value. In principle this perturbation is quasi-inertial pointing but since the plant is based on a LVLH formulation, the orbital rotation velocity is used to set the cross-over frequency of the W_d function.

  With a normalised magnitude of 1 for input *d* and sub-mm pointing precision at output z_1, the corresponding suppression value can thus be computed leading to a requirement on W_S.

- Gravity gradient suppression: By far, the most important perturbation is the gravity gradient, i.e. the relative orbital dynamics. Rather than treating this as a pure external perturbation, it is treated as part of the plant model. The farther the OSC is located from the CSC, the stronger the gravity gradient, the stronger the controller's integral action needs to be.

  The ISD will determine the magnitude of the gravity gradient and this information is introduced via the channel from *r* to z_1. The ratio of the sub-mm performance and ISD value will thus impose a suppression requirement on W_S.

  In the FSK phase, the formation is (quasi) inertial so the tracking reference r "rotates" with the local orbital velocity wrt to the plant's orbital frame. Consequently, the orbital rate is used to set the frequency range of the desired suppression in W_S. (Note, however, that this may lead to an artificially conservative criterion due to the chosen reference frame).

- Retargeting manoeuvres: During the reorientation of the formation, which is performed at a rate of 30 deg in 2 hours, the "rotation" of the tracking reference *r* increases but it is accompanied by a reduced suppression factor due to the relaxed performance in HPM. The function W_S will thus contain a desired suppression factor, which is lower than that of the nominal FSK with HPAP performance, but at a higher frequency.

  Note: As it turns out, the retargeting manoeuvre requirement is the bigger driver of the two.

- Navigation noise level: Currently, no definitive data is available for the Navigation errors with high accuracy metrologies. Consequently, some assumptions are to be made. The magnitude is assumed to be compatible with the mm-level position accuracy. Since the Navigation uses explicit attitude information, it is here assumed for simplicity that the noise frequency range may go down to the attitude controller bandwidth, which is provided by the responsible design party in question.

In any case, the results show that the noise input does not drive the synthesis as the associated input/output norms are small.

- Control error signal smoothing: As mentioned above, the weighting function W_{KS} can be used for adding additional poles and zeros, which can be useful for noise filtering of the error signal. The thruster PWM frequency (0.05Hz) is lower than the control frequency (1Hz), which will lead to a thruster specific signal noise within the control error signal that may in theory deteriorate the control output signal. To reduce this negative effect, the W_{KS} function is explicitly tuned to impose some low-pass filtering of the error signal.

The synthesis is done in MATLAB using the Robust Control Toolbox. The block diagram in Fig. 2 is reorganised as shown in Fig. 3 and the augmented generalised plant *P* is obtained for the H_∞ framework.

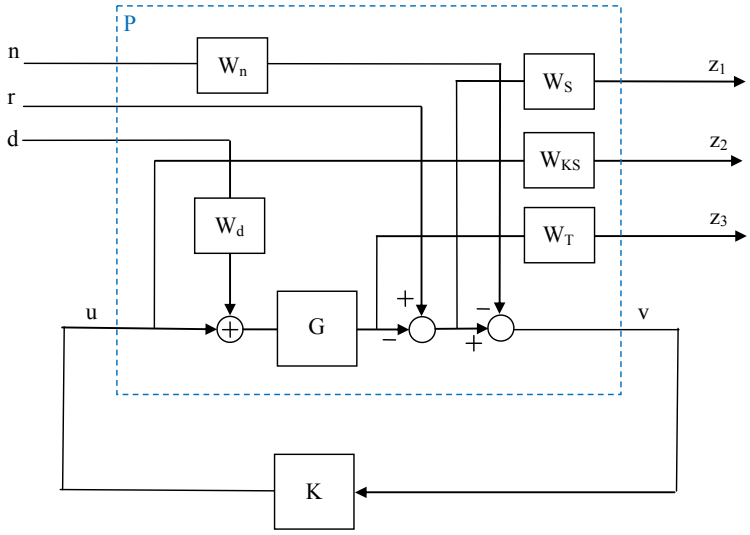

Fig. 3: Block diagram of the generalized plant for controller synthesis

A minimum realisation (i.e. minimum number of states) of the state space model of the generalised plant *P* is obtained symbolically where the individual state-space matrices of the spacecraft plant *G* and weighting functions W_i are explicit parameters in Eq. (1) and Eq. (2). These equations allow easy and fast design iterations and testing as the weighting functions can be retuned and altered at will as the resulting minimum realisation state-space model of the generalised plant is obtained immediately for each case.

Due to the nature of the relative orbital mechanics and chosen reference frame, the state-space model is separated into an out-of-plane model and an in-plane model. The former is a SISO system (Single Input Single Output) whereas the latter is a MIMO system (Multiple Input Multiple Output) where the two axes are dynamically cross-coupled.

$$\dot{\bar{x}} = \begin{bmatrix} A_d & 0 & 0 & 0 & 0 & 0 \\ B_G C_d & A_G & 0 & 0 & 0 & 0 \\ B_T D_G C_d & B_T C_G & A_T & 0 & 0 & 0 \\ B_S D_G C_d & B_S C_G & 0 & A_S & 0 & 0 \\ 0 & 0 & 0 & 0 & A_n & 0 \\ 0 & 0 & 0 & 0 & 0 & A_{KS} \end{bmatrix} \bar{x} + \begin{bmatrix} 0 & B_d & 0 & 0 \\ 0 & B_G D_d & 0 & B_G \\ 0 & B_T D_G D_d & 0 & B_T D_G \\ B_S & -B_S D_G D_d & 0 & -B_S D_G \\ 0 & 0 & B_n & 0 \\ 0 & 0 & 0 & B_{KS} \end{bmatrix} \begin{pmatrix} \bar{r} \\ \bar{d} \\ \bar{n} \\ \bar{u} \end{pmatrix} \quad (1)$$

$$\begin{pmatrix} z_1 \\ \bar{z}_2 \\ \bar{z}_3 \\ \bar{v} \end{pmatrix} = \begin{bmatrix} D_S D_G C_d & D_S C_G & 0 & C_S & 0 & 0 \\ 0 & 0 & 0 & 0 & 0 & C_{KS} \\ D_T D_G C_d & D_T C_G & C_T & 0 & 0 & 0 \\ D_G C_d & -C_G & 0 & 0 & -C_n & 0 \end{bmatrix} \bar{x} + \begin{bmatrix} D_S & D_S D_G D_d & 0 & -D_S D_G \\ 0 & 0 & 0 & D_{KS} \\ 0 & D_T D_G D_d & 0 & D_T D_G \\ I & -D_G D_d & -D_n & -D_G \end{bmatrix} \begin{pmatrix} \bar{r} \\ \bar{d} \\ \bar{n} \\ \bar{u} \end{pmatrix} \quad (2)$$

The synthesis results are shown in Fig. 4 to Fig. 7 where the maximum value of the Singular Value Decomposition (SVD) of the channels from r to z_i and d to z_1 are shown (as blue lines) together with the corresponding weighting functions (as red lines). Each of the channels is a 3x3 MIMO transfer function. The resulting H_∞ norm of the complete transfer function from all inputs to all outputs is equal to $\gamma = 0.89$. In these figures, the controller transfer functions are already subjected to an order reduction, which is a common procedure as the H_∞ synthesis routine tends to generate a high order function, which ought to be reduced without affecting the desired controller properties.

Of special interest is Fig. 5 where the suppression factor via the boundary W_S is obtained. In this figure, the grey area represents the forbidden area that the resulting controller may not enter. The two corner points at the lower left side represent the suppression requirements of the HPAP performance during nominal FSK and the HPM performance during the retargeting manoeuvres. It can be observed that it is the latter that drives the controller design.

An interesting observation is that the low frequency suppression boundary W_S (see red line) does not go down towards the underside of the grey area, which one would expect it to do. This is done on purpose. The required suppression factor is very stringent and a 3rd order transfer function for W_S was necessary to achieve the desired goal. But still, having the lower plateau of the inverse of W_S under the grey area would lead to a lower limit in bandwidth imposed by W_S that would violate the upper bandwidth restriction imposed by W_T in Fig. 4. Increasing the order of W_S to obtain a steeper slope was considered too extreme as that would affect the controller design negatively. Instead, the solution was found by altering the weighting function Wd.

Figure 7 shows the I/O channel from disturbance d to output z_1. Here, the grey area represents the forbidden area meaning that the differential solar radiation pressure will be rejected by the controller as long as that grey area is not crossed. As can be observed, there is ample margin but that is due to the fact that W_d, i.e. the function that contains the information on the solar radiation pressure's magnitude and frequency range, has artificially been increased. By doing so, the synthesis procedure would then force a stronger suppression factor, which caused the blue line in Fig. 5 to successfully go under the grey area by falling steeper according to the chosen cross-over frequency in W_d without violating the boundary limits set by W_S and W_T. This is a good example

that shows that one cannot blindly press the button and expect the synthesis routine to come with the desired solution. In fact, some artisan engineering was in order.

Figure 6 shows the function *KS* and its corresponding boundary. The function W_{KS} has been tuned iteratively such that the peak of *KS* "touched" the boundary in which case some poles were forcefully added at the desired frequencies to the controller transfer function for filtering purposes.

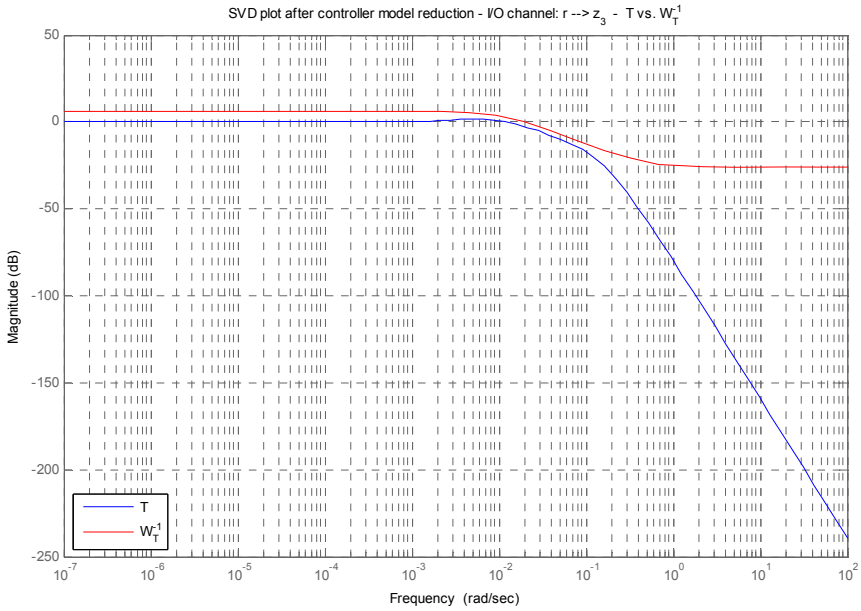

Fig. 4: SVD plot of *T* vs the inverse of W_T

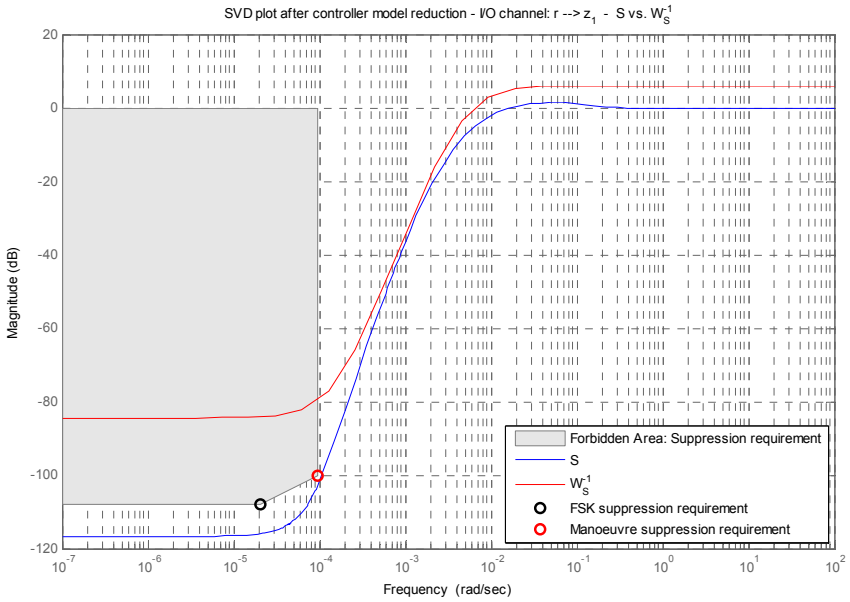

Fig. 5: SVD plot of *S* vs the inverse of W_S

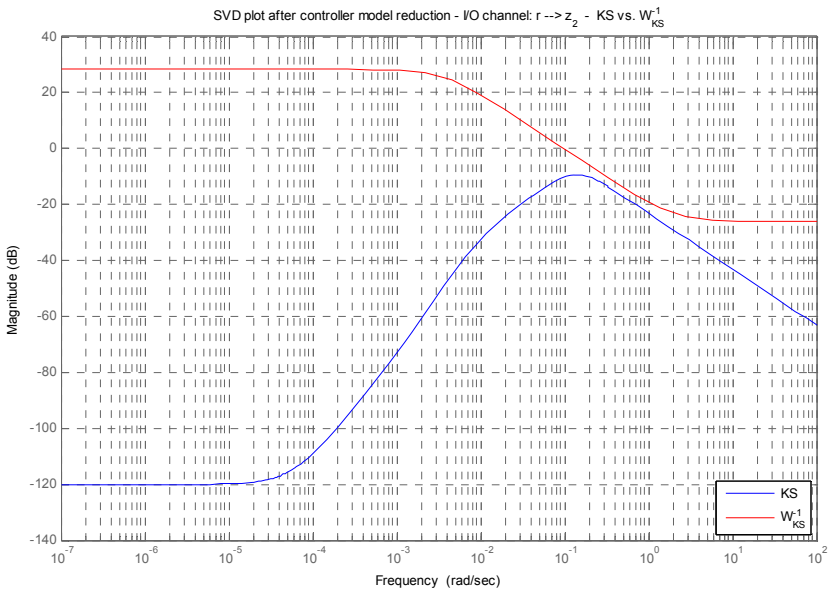

Fig. 6: SVD plot of *KS* vs the inverse of W_{KS}

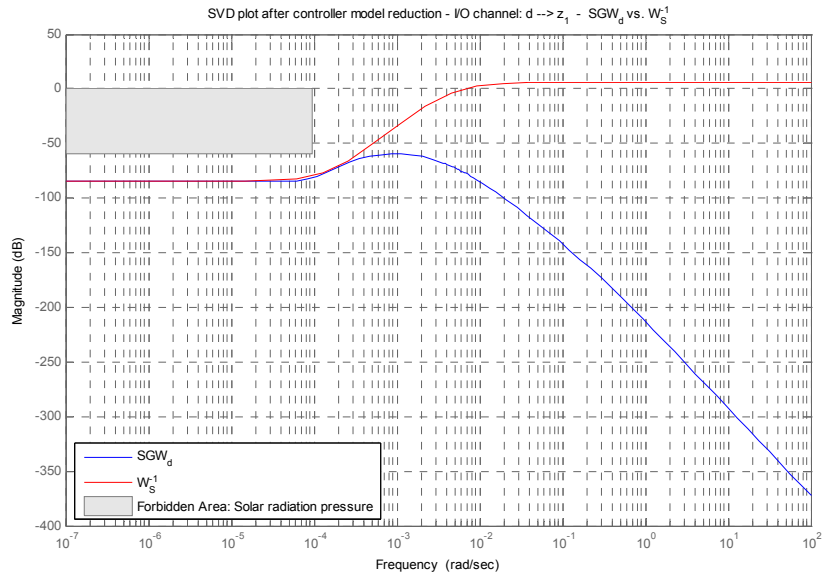

Fig. 7: SVD plot of SGW_d vs the inverse of W_S

2.6. Analysis with plant variations

The reference LTI plant model is based on a particular point on the orbit. After synthesising the controller, a check is performed where the SVD results of the relevant functions are recomputed with LTI plant models corresponding to various points covering the orbital arc around the apogee in which the flight-formation is active. The results are shown in Fig. 8 and it can be seen that the boundaries are indeed not violated.

2.7. Stability margins

The classical gain and phase margins are mainly applicable to SISO systems and they tend to lose significance in strongly coupled MIMO systems. However, considering the dominant diagonal structure of the controller, they can still be applied here providing relevant information. Plus, the out-of-plane controller is part of a SISO system anyway due to the decoupling property of the chosen plant dynamics. Note that for the MIMO in-plane controller, when creating the open loop system for one axis, the other axis is maintained in closed loop acting as an internal dynamical system.

The corresponding stability margins are: 10.5 dB gain margin and 48.5 deg phase margin for all axes. Sufficient phase margin is considered important considering a thruster PWM period of 20 seconds and an inter satellite link latency of 3 seconds. After all, the CSC contains the optical metrology for the relative position measurements that are sent to the OSC, which contains the navigation filter.

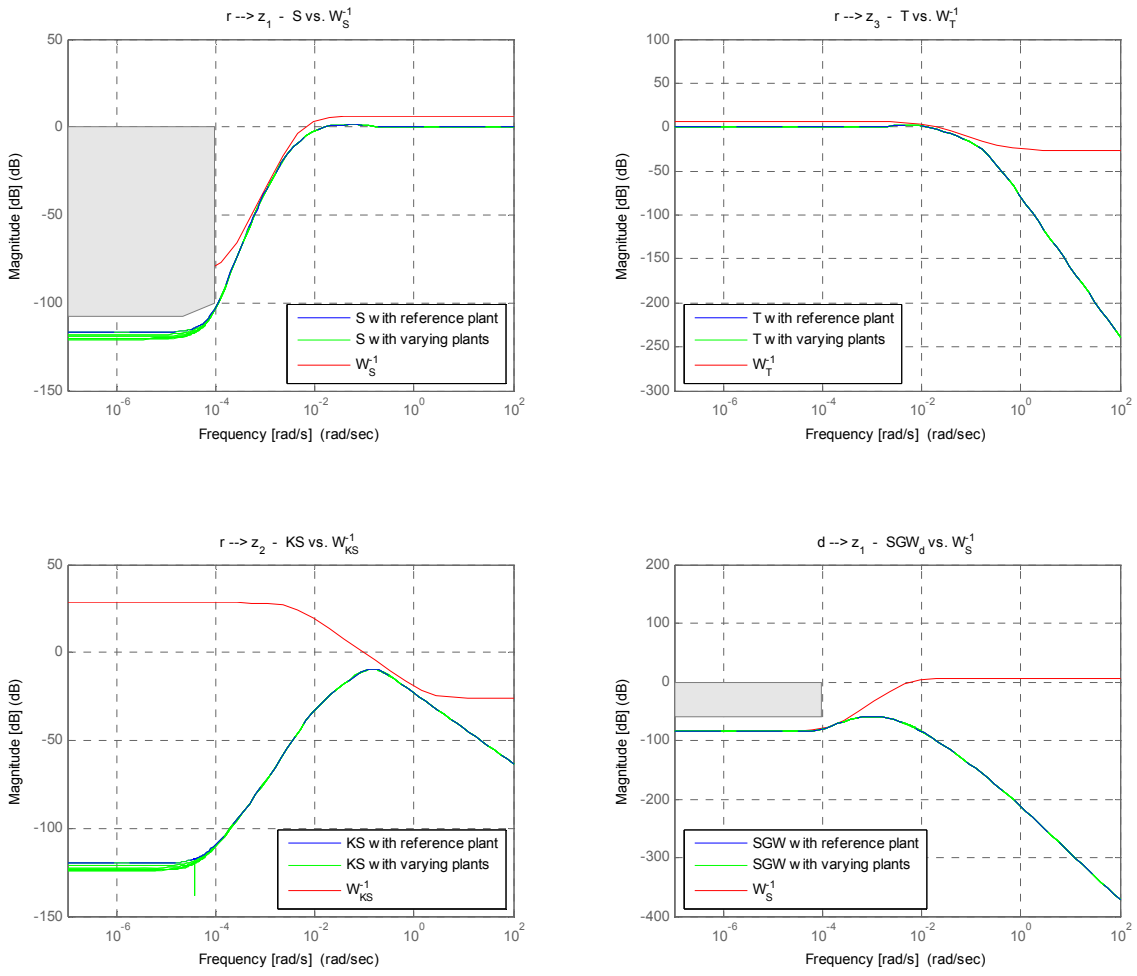

Fig. 8: Analysis with varying plant models

2.8. Non-linear time-domain simulations

The results need to be validated in a non-linear time-domain simulator. Officially, this needs to be done in the PROBA-3 FES (Functional Engineering Simulator) where all contributions of all the involved parties are present. But naturally, prior to delivery to the FES, the controller needs to be tested first in a standalone simulation environment. For this purpose, a dedicated simulator has been created based on SENERic, which is a high fidelity in-house developed configurable simulation environment in MATLAB/ SIMULINK.

This validation simulator consists of the following properties:

- Full 6DoF dynamics
- Two independently propagated orbits to simulate the flight formation
- Gravity field (EGM96) for representative gravity gradients
- ISD of 150m
- Inter satellite delay link (3 sec) in the control loop
- Functional attitude controller to simulate the SC-GNC
- Simplified yet functional Navigation module → 0.12 mm (1σ) Gaussian noise at 1Hz (according to expected filter performance)
- Simplified yet non-linear thruster system → force per axis →but with a representative PWM scheme at 0.05Hz and minimum on-time of 50 msec

It should be mentioned that the attitude control and Navigation filter are provided by other parties (NGC and GMV respectively) and consequently these modules are not available for use in SENERic and functional substitutes were developed in order to be able to perform these required standalone validation tests.

The simulation test setup consists of simulating first the acquisition phase prior to the FSK phase, which is performed by the Coarse Acquisition Control, which is not covered in this paper. Once the desired sub-cm accuracy is obtained, then the High Performance Control, i.e. the H_∞ synthesised control as presented in this paper, takes over with the objective of meeting the stringent HPAP performance requirements. The results are shown in Fig. 9 where the transition to the High Performance Control occurs at t = 2000 sec.

The controller is implemented as a discrete state-space model running at the FF-GNC frequency of 1Hz. The afore mentioned feed-forward term to compensate the gravity gradient is deliberately omitted in this test in order to assess the feedback control performance without any aid.

These results show that the positioning accuracy is well below 1 mm hence the designed controller is able to cope with the relative orbital dynamics and the non-linear thruster PWM effects. By choice, any systematic error is deliberately excluded in this particular test in order to assess the control performance in the presence of temporal error contributions that are “observable” by the controller.

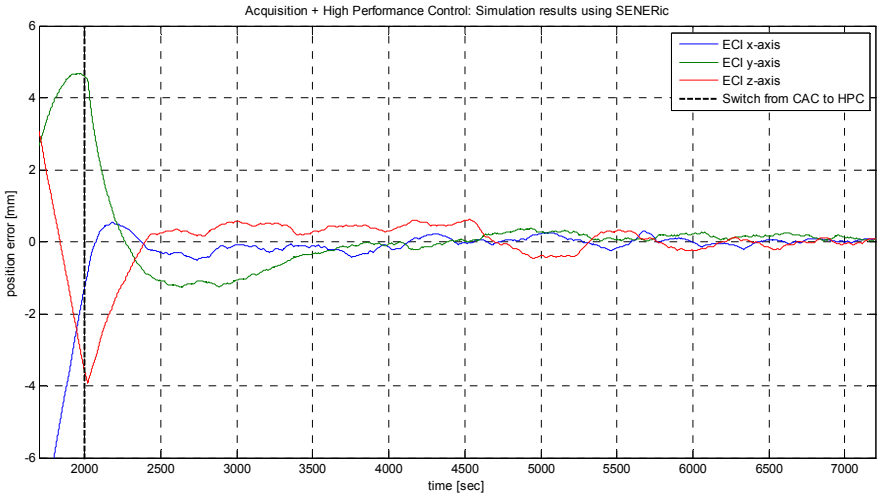

Fig. 9: Non-linear time domain simulation test

3. Conclusion

An H_∞ MIMO controller has been designed and successfully tested in a representative simulation setup and thereby demonstrating the feasibility of the PROBA-3 flight-formation scenario with stringent performance requirements.

The spacecraft plant dynamics are expressed in a LVLH frame and based on the relative orbital dynamics for elliptical orbits as provided by the Yamanaka-Ankersen equations in Reference [2]. Rather than particularising for the quasi-inertial PROBA-3 flight-formation, this design approach has the advantage of being more general and applicable to other flight-formation scenarios, which is of relevance since one of the objectives of PROBA-3 is to obtain a design methodology that can be applied to other future missions.

A MIMO control has been obtained that successfully meets the requirements for nominal performance and stability and in the next phase, robustness properties such as RP, RS, attitude and position cross-coupling, etc., shall be address and analysed in more depth.

References

[1] J. Peyrard, C. De Negueruela, T. V. Peters, C. Carrascosa, A. Agenjo, and R. Sánchez. “The GNC System of PROBA-3”. Proceedings of 4th International Conference on Spacecraft Formation Flying Mission and Technologies, held on St-Hubert, Québec (Canada).

[2] New State Transition Matrix for Relative Motion on an Arbitrary Elliptical Orbit. K. Yamanaka, F. Ankersen. Journal of Guidance, Control And Dynamics Vol.25, No.1, Jan-Feb 2002